

microfractures are few in number, they are strongly oriented subnormal to  $\sigma_3$  and nearly parallel to  $\sigma_1$ ; that is, they are extension fractures (fig. 5, *a*).

*Specimen 915.*—Three sets of twin lamellae are developed with an average spacing index of 212. Fractured detrital grains are found throughout the specimen, and the fracture index (219) is markedly higher than that of specimen 878. Moreover, the microfractures tend to lie perpendicular to  $\sigma_3$  (fig. 5, *b*). No shear zone is developed.

*Specimen 877.*—Three sets of twin lamellae are developed with an average spacing index of 297. Microfractures occur throughout the specimen, and again are oriented as extension fractures (fig. 5, *c*). The fracture index (212) probably represents a minimum value (see table 1, n. §). A macroscopic shear zone inclined at  $38^\circ$  to  $\sigma_1$  was observed prior to sectioning. Three instances of intragranular internal rotation were observed in this specimen; that is, the twin lamellae formed early were rotated to irrational positions by twin gliding on another set of lamellae formed later in the deformation. Since the position of  $\sigma_1$  is known in the experiment, it is possible to calculate the average strain of each specimen (Turner, Griggs, and Heard, 1954, p. 900). The strains in the three different fields of view are 6.8, 7.6, and 10.6 per cent, respectively—average, 8.3 per cent. The total strain, measured experimentally, is 8.5 per cent.

*Specimen 911.*—The same fabric elements that characterize the other specimens are more strongly developed in specimen 911 (pl. 1). From bottom to top, the specimen can be divided into slightly deformed, moderately deformed, and highly deformed areas. The calcite crystal within the slightly deformed and moderately deformed areas exhibits three sets of twin lamellae. The spacing index of each of these sets varies from one field of view to another, but usually the three sets are equally well developed; the average index is 315. The index increases toward the highly deformed, necked portion of the specimen. In any field of view, the index of a given twin set tends to be greater

near the detrital-grain boundaries than in the central portion of an interstitial area (pl. 2*B*, *d*). In the highly deformed area calcite is characterized as follows:

1. Three twin sets are recognizable, although spacing of lamellae is predominantly dense, that is,  $>400$  per mm. Undulatory extinction and bent lamellae are common.
2. Narrow areas of very fine-grained calcite gouge have developed along shear zones.
3. A very fine- to fine-grained mosaic of granulated calcite—a deformation mosaic—has developed throughout the area.

The detrital grains are fractured (index 288), except for those in the triangular area at the base of the cylinder in the "shadow" of the end cup (pl. 1). Except for demolished grains, most quartz, feldspar, and garnet grains and rock fragments exhibit one set of many subparallel microfractures. The microfracture surfaces are strikingly planar (pl. 2*B*, *a*, *b*, and *c*). The number of microfractures per set increases from slightly deformed to moderately deformed to highly deformed areas; in the highly deformed portion, "demolished" grains are commonly smeared out along shear zones. Most microfractures completely cross the host grain, but they may die out within the grain. A  $5^\circ$ – $15^\circ$  rotation of fragments between microfracture surfaces can sometimes be seen if the host grain is at extinction. This phenomenon and the play of light on the microfracture surfaces cause some grains to exhibit "pseudolamellae" of slightly different optical orientation.

The angular relationship between the normals to microfracture surfaces and the  $c_v$  of the host quartz grains is illustrated in figure 6. There is a slight tendency for the surfaces to parallel  $r$  or  $z$ . That this relationship is non-random may be demonstrated by comparing the histogram with one representing random distribution as shown in figure 6, *a*.

The microfractures show a strong tendency to lie perpendicular to the known position of  $\sigma_3$  (fig. 7). The few microscopic shear zones occur at approximately  $30^\circ$  to  $\sigma_1$  (pl. 1 and 2*B*, *c*).

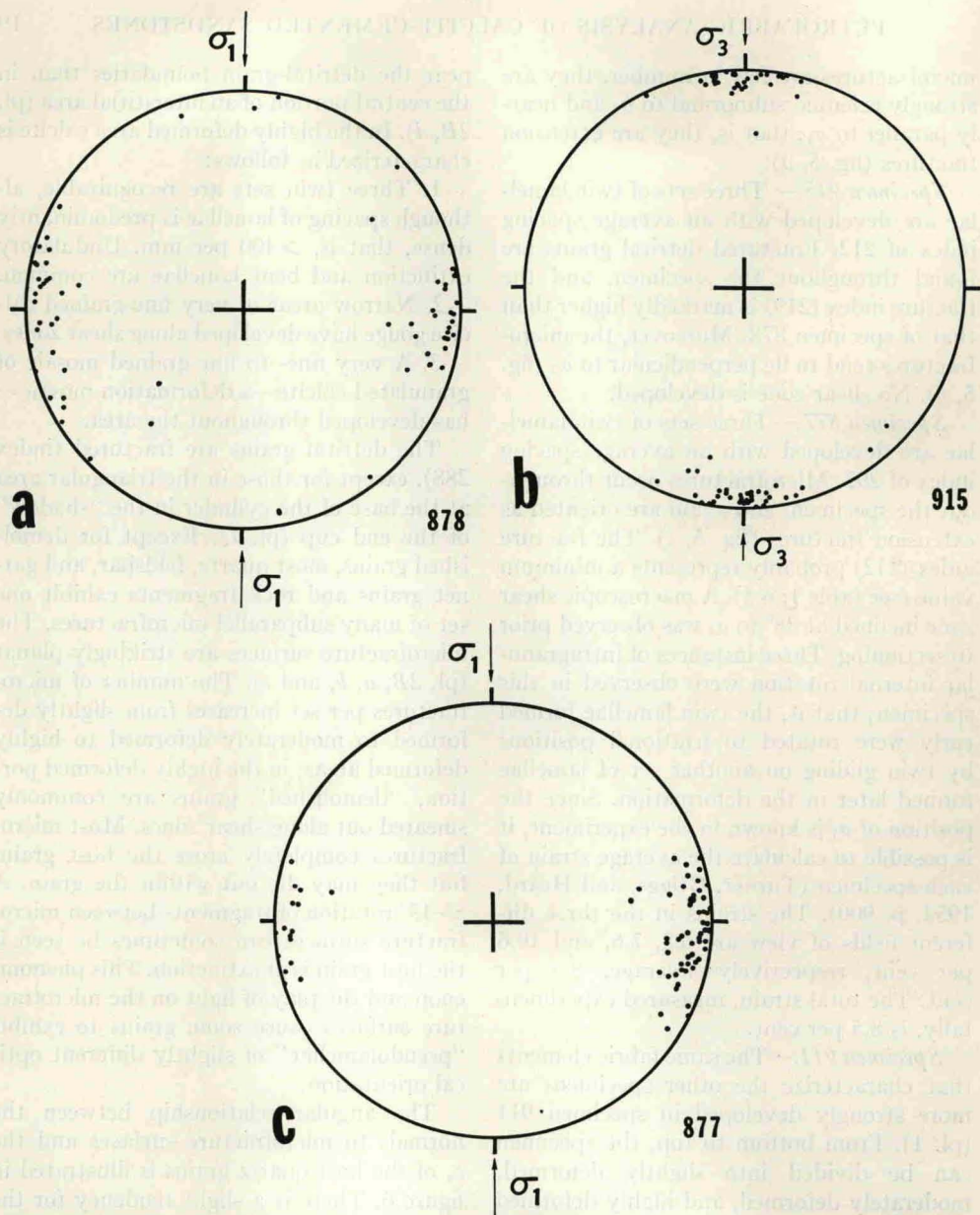


FIG. 5.—Diagrams illustrating orientation of microfractures with respect to load axis for specimens 878, 915, and 877. Plane of each diagram is parallel to long axis of deformed cylinder. *a*, specimen 878, normals to 63 sets of microfractures in fifty detrital grains. *b*, specimen 915, normals to 64 sets of microfractures in fifty detrital grains. *c*, specimen 877, normals to 69 sets of microfractures in fifty detrital grains.

PLATE 1

Photograph shows thin section cut parallel to the axis of deformed, necked cylinder.  $\sigma_3$  is vertical, and  $\sigma_1$  is horizontal. Area of thin section is approximately one-half of total specimen; i.e., cylinder broke just above the necked region when removed from its copper jacket. Planar fractures in detrital grains are oriented predominantly perpendicular to  $\sigma_3$ , and twin lamellae in the calcite crystal are visible. Slightly deformed, moderately deformed, and highly deformed sectors of the cylinder are indicated. Crossed nicols,  $\times 10$ .